Rapid Communications

Energy spectrum in the dissipation range

Sualeh Khurshid and Diego A. Donzis*
Department of Aerospace Engineering, Texas A&M University, College Station, Texas 77843, USA

K. R. Sreenivasan
Department of Mechanical and Aerospace Engineering, Department of Physics, and Courant Institute of Mathematical Sciences, New York University, New York, New York 10012, USA

(Received 15 June 2018; published 8 August 2018)

We study the dissipation range of the turbulent energy spectrum in homogeneous and isotropic turbulence via highly resolved direct numerical simulations for microscale Reynolds numbers R_λ between 1 and 100. The simulations resolve scales as small as a tenth of the Kolmogorov scale. We find that the spectrum in this range is essentially exponential for R_λ up to about 20, but assumes a more complex form for higher R_λ. This shape can be regarded roughly as a superposition of two exponentials where the second exponential, which becomes stronger with increasing R_λ, appears to be the result of intermittent interactions with the lower wave-number part of the spectrum; it disappears when these interactive parts are filtered out before computing the spectrum, essentially recovering the initial exponential shape. The multifractal theory accounts for better collapse in a limited range of wave numbers up to Reynolds numbers of 1000 observed with additional simulations at lower resolutions.

DOI: 10.1103/PhysRevFluids.3.082601

Kolmogorov's seminal work (K41) [1] assumed that the energy spectrum of turbulent fluctuations at dissipative scales (around and beyond the so-called Kolmogorov scale $\eta \equiv \nu^3/\langle\epsilon\rangle^{1/4}$) is determined solely by the mean energy dissipation rate ($\langle\epsilon\rangle$) and the kinematic viscosity (ν). This insight gave rise to a flurry of models by Obukhov, Heisenberg, von Kármán, Kovasznay, and others. These early models (see Sec. 17 of Monin and Yaglom [2]) were essentially dimensional arguments containing additional hypothesis and were "more or less speculative and lacking sound physical bases" (see Ref. [2], p. 212). A different line of theoretical attempts was initiated by Kraichnan [3] via his direct interaction approximation, which argued that the spectrum must be an exponential. The result in a somewhat more general form is given by

$$E(k\eta) \sim (k\eta)^\alpha e^{-\beta(k\eta)^\gamma} \tag{1}$$

for wave numbers k in the range $k\eta > 1$. Other authors [4–8] have arrived at similar forms by different and independent reasoning. In the form (1), the equation has been tested by a number of authors using direct numerical simulations (DNS) [9–13]. Measurements have rarely resolved past the Kolmogorov scale.

Optimal fitting of Eq. (1) to the DNS data is not straightforward because three free parameters are involved in a strongly nonlinear form. A major assumption in most studies is to put $\gamma = 1$, leaving only two coefficients to be determined. Under this assumption, Chen *et al.* [10] found $\alpha \sim 3.3$ and $\beta \sim 7.1$ for $R_\lambda \sim 15$ within the range $5 < k\eta < 10$. Martinez *et al.* [11] improved on this work by

*donzis@tamu.edu

 ©2018 American Physical Society

TABLE I. Summary of DNS runs. N is the number of grid points in each direction. ΔT_E is the number of eddy turnover times in the stationary state. The upper limit on the far-dissipation range is determined by the smaller number between $k_{\max}\eta$ and $k\eta$ near the round-off limit.

R_λ	N	$k_{\max}\eta$	ΔT_E	NDR	FDR
1	128	53.7	9.06	2.5–6	6–14
3	128	30.5	13.6	2–6	6–12.5
7	128	17.8	15.9	2–6	6–11
9	256	28.1	11.8	1.5–4.5	8–11.5
10	512	55.6	10.2	2–4	8–11.5
14	256	20.7	7.38	2–4	8–12
19	512	34.7	9.93	2–4	8–11
25	256	12.3	19.6	2–4	8–11.1
47	1024	24.8	19.2	2–4	8–12.5
55	1024	19.9	18.4	1.5–3	8–11.7
68	1024	14.9	19.3	1.5–3	8–12.9
89	2048	21.2	24.2	1.5–3	8–13.7

studying a range of R_λ. They locally fitted the log-derivative of Eq. (1), $\phi(k\eta)$, which has the form

$$\phi(k\eta) \equiv \frac{d\ln[E(k\eta)]}{d\ln(k\eta)} = \alpha - \beta\ \gamma\ (k\eta)^\gamma. \tag{2}$$

Their highest resolved simulation suggested two scaling ranges below and above $k\eta \sim 4$ and indicated that a simple exponential may not be appropriate. Ishihara *et al.* [12] fit the near-dissipation region for Eq. (1), but for R_λ higher than those of Ref. [11]. Both papers show a R_λ dependence for α and β. Schumacher *et al.* [13] performed an analysis similar to Ref. [11] using higher-resolution data and reported that no unique set of parameters exists, though they also noted a saturation in the values of these parameters around $R_\lambda \sim 100$.

Most previous studies did not include large ranges of R_λ, or concerned themselves with low values of R_λ, or have resolved scales not too far into the dissipation range. To some degree, this accounts for the variety of conclusions. It seemed desirable to extend both the Reynolds number range and the resolution of the simulations and obtain more conclusive results on the spectral shape in the dissipative region. This is the goal of the present study. We perform DNS with very fine resolution, as detailed in Table I, for R_λ ranging from 1 to about 100. The code is pseudospectral and uses a Runge-Kutta scheme (RK2) for time integration. The time step is 3–80 times smaller than the Kolmogorov timescale in the stationary state Courant-Friedrichs-Lewy (CFL) range: [0.1–0.7]. The flow is forced in Fourier space with integrated Ornstein-Uhlenbeck processes [14] with a finite-time correlation at the largest scales within the sphere $k < 2.01$. The Reynolds number is changed by changing the viscosity. In all cases, the highest resolvable wave number $k_{\max} = \sqrt{2}N/3$ (N being the number of grid points in each direction) is at least an order of magnitude larger than the Kolmogorov scale. The stationary state averaging is started at least six eddy turnover times from the initial conditions. We have tested for potential numerical artifacts caused by finite-arithmetic precision or truncation, aliasing errors, and numerical differentiation schemes, and have shown that these effects do not influence the results (see the Appendix).

In Fig. 1(a) we collect spectra for a range of Reynolds numbers. From a quick look, the data show an approximate collapse at all Reynolds numbers, as expected from classical phenomenology; interestingly, this rough collapse seems to cover even very low Reynolds numbers of $\sim O(1)$. A more careful inspection of the spectra, however, reveals two important departures from the self-similarity implied in K41. First, spectral collapse is not strictly achieved at the low end of the dissipation range, say, $k\eta \sim 0.1$–1, as seen better on the linear scale of the inset [Fig. 1(a)]. As pointed out in Ref. [15], there is a clear systematic decrease of this so-called bottleneck effect (the spectral

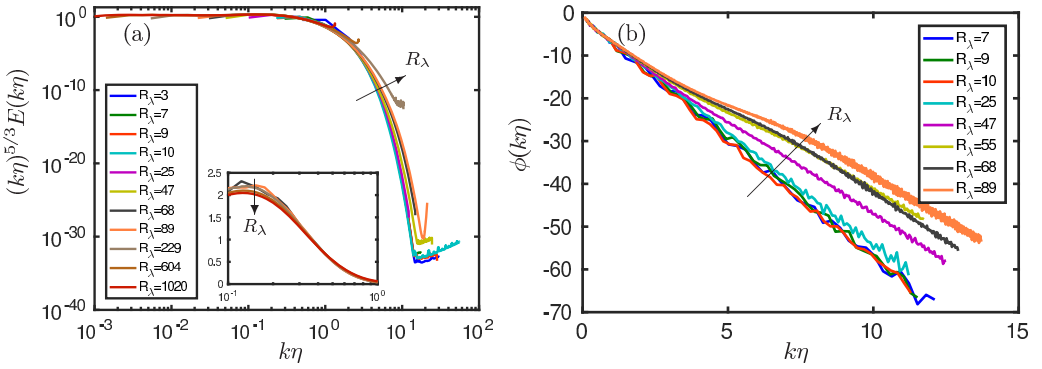

FIG. 1. (a) Energy spectrum for all R_λ in the database. Inset: Detail of $(k\eta)^{5/3}E(k\eta)$ for $R_\lambda \gtrsim 50$. Data for $R_\lambda > 89$ are taken from Ref. [15]. (b) The log-derivative $\phi(k\eta)$ for very well-resolved simulations shows two ranges. Selected R_λ are shown to reduce clutter and illustrate the trend.

bump that precedes the dissipative region at $k\eta = 0.13$) with the Reynolds number; this can also be observed in the data of Ref. [16]. Second, and this is the focus of the present Rapid Communication, one can also see persistent systematic trends with the Reynolds number even at higher wave numbers; see Fig. 1(b). Several previous simulations did not observe or emphasize this aspect. The observed behavior cannot be fitted by an exponential over the entire range and, indeed, the shape of the data precludes the applicability of spectral formulas such as Eq. (1).

Nevertheless, it appears useful to consider the spectral shape to consist of two exponentials with an extended crossover, the near-dissipation range (NDR), $k\eta \lesssim 3$, and the far-dissipation range (FDR), $k\eta \gtrsim 6$, for each of which one may be able to fit Eq. (1), but with a different set of constants. This approach is in contrast to virtually all theoretical models which predict, for $k\eta \gg 1$, the general form Eq. (1), sometimes with a sum of more than one power law in the prefactor [3,9]. Although no rigorous argument has been put forth for multiple exponentials, there have been some efforts to use Eq. (1) with different coefficients in different ranges—for example, Ref. [11], though their simulations did not resolve far enough into the FDR to reliably obtain the coefficients and their fits used $\gamma = 1$, which does not apply. There has also been some recent theoretical work on chaotic systems which may justify the appearance of multiple exponentials [17].

To compute the coefficients we first plot the log-derivative of the normalized energy spectrum, compensated with $\gamma(k\eta)^\gamma$, such that Eq. (2) yields

$$\frac{\phi(k\eta)}{\gamma\ (k\eta)^\gamma} = \frac{\alpha}{\gamma\ (k\eta)^\gamma} - \beta. \tag{3}$$

If $\alpha = 0$, for instance, even for a limited range of $k\eta$, a constant β would result and γ can be determined by searching for the value that results in the widest plateau of the left-hand side of Eq. (3).

For R_λ up to about 10 (perhaps even 20), Fig. 1(b) shows that $\gamma = 1$ approximates the data well which in this figure would be seen as a straight line; we then obtain $\beta = 6.7$, similar to Refs. [10,11]. A few remarks are in order for determining the constants for larger R_λ. First, past efforts have generally used a fixed value of γ and used a finite nonzero value of α. But fixing γ at a predetermined value can only lead to incorrect values for the coefficients, as seen clearly in Fig. 1(b). Second, the optimization procedure that can be used to find the best fit coefficients by minimizing the error between DNS and Eq. (1) leads to a number of challenges for finding the global minimum in the error, because of the strongly nonlinear nature of the procedure. Standard techniques typically find local minima strongly dependent on the initial seeds. In any case, such efforts in NDR and FDR generally give values of α that are relatively small, fluctuating inconsistently around zero, from which one can justify setting $\alpha \approx 0$ without any loss of accuracy of fits. This conclusion is reinforced from typical compensated

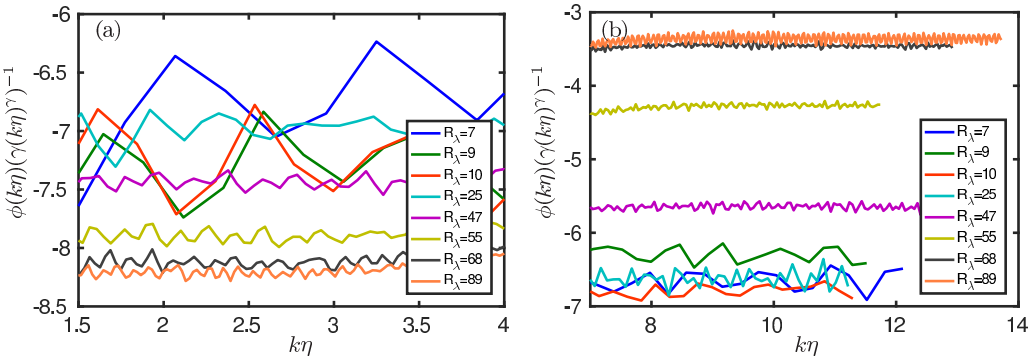

FIG. 2. The compensated log-derivative for (a) NDR and (b) FDR of the energy spectrum.

log-derivatives shown separately in Fig. 2 for NDR and FDR, whose extent (by visual inspection) is summarized in Table I: One can see clear plateaus in Fig. 2, rather than an asymptotic approach to plateaus at high $k\eta$ as would be the case if $\alpha/[\gamma(k\eta)^\gamma]$ is not negligible. This plateau effect can be due either because $\alpha \approx 0$ or because $k\eta$ is high enough to make that term negligible. In both cases, the conclusion is that the value of α is largely inconsequential in both the NDR and FDR (see also the Appendix). This is consistent with the extreme sensitivity in determining α from fits including only $k\eta \gtrsim O(1)$ using standard minimization tools.

A phenomenological argument for including the power-law term with nonzero α is essentially that the exponential roll-off in the dissipation range must transition smoothly to a power law in the inertial range with an exponent of $-5/3$ [1]. However, it is now well established that the dissipation and inertial ranges are separated by a spectral bump due to the bottleneck effect [15,19]. This realization has led to the use of varying power laws as prefactors [9,20]. However, as argued above, a simple sensitivity analysis of the fitting parameters reveals that changes in α do not significantly affect β. We thus put $\alpha = 0$ in NDR and FDR but accept two different γ values in each of the regions.

Still, if one insists on using a finite, nonzero α, the present data indicate that the effect is relatively small because of the clear plateau observed in the compensated log-derivative seen in Fig. 2, which implies that the first term in Eq. (3) is indeed small. The observed plateaus can be used to estimate bounds on α. Requiring that the second term be much larger (needed for a plateau), say, an order of magnitude larger than the first, requires (using the fact that $\beta\gamma \approx 6.4$—see below) that $\alpha \ll 0.1\beta\gamma(k\eta)^\gamma \approx 0.64$ in the NDR and $\alpha \ll 2.4$ in the FDR; the observed plateaus actually suggest that α is much smaller.

Once γ is known, it is straightforward to determine α and β (or only β) using standard minimization tools. The values of γ found using the compensation method detailed above which led to the plateaus observed in Fig. 2 are collected in Fig. 3(a). At low R_λ, γ is slightly smaller than 1 for both NDR and FDR, but it is hard to assign any deep significance to the observed difference from unity. At higher Reynolds numbers, however, we see the emergence of the two ranges. In the NDR, γ decreases with increasing R_λ and remains below 1. With these values of γ we performed least-squares fits to determine β. The results are shown in Fig. 3(b). Here, too, we observe different behaviors for the two ranges of the spectrum when $R_\lambda \geqslant 10$. The parameter β increases with increasing R_λ for the NDR but decreases for FDR. An interesting result in the NDR is that $\beta\gamma$ is fairly constant around 6.4 for all R_λ studied here.

In contrast to K41, multiple dissipation ranges are predicted by the multifractal formalism [18], which assumes a local scale invariance rather than the global scale invariance of K41. This manifests as a scaling of velocity increments with a Hölder exponent h within an interval $(h_{\min}, h_{\max})$; for each h, a fractal set with dimension $D(h)$ can be determined [18]. Scaling exponents are turned off successively as viscosity becomes increasingly important at higher k. In doing so, a new similarity parameter $\theta = \ln(k\eta)/\ln(R_\lambda)$ is derived such that $\ln[E(k\eta)]/\ln(R_\lambda) \equiv f(\theta)$. In Fig. 4, we show

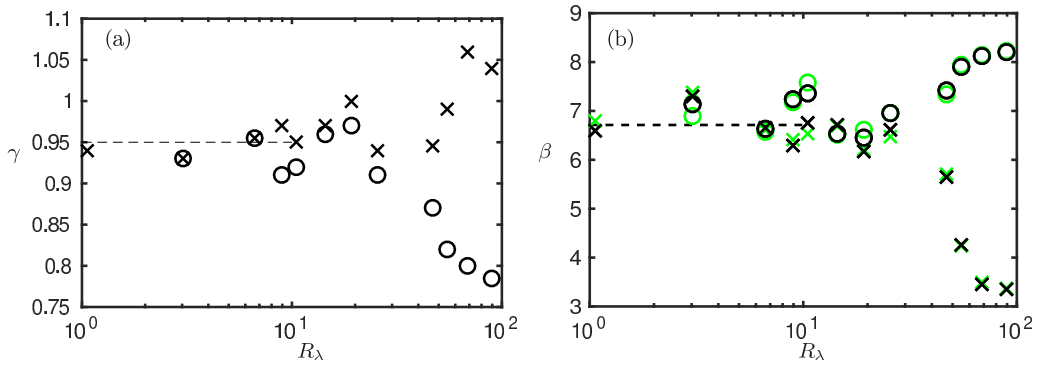

FIG. 3. (a) Values of γ as a function of R_λ found from the compensated log-derivative form as described in the text. NDR values are represented by $\circ$ and FDR by $\times$. (b) The constant β after fitting Eq. (3) for appropriate γ as a function of R_λ. Symbols $\circ$ and $\times$ are from NDR and FDR fits, respectively. Black symbols correspond to fits with $\alpha = 0$ and green for fits with α as a fit parameter. The 2-norm of relative error between DNS data and the fit (not shown) is less than 4% and decreases with increasing R_λ. No significant improvements in relative error are observed with the inclusion of α in the fit.

the log-derivative of the energy spectrum in the new variables which has a more compelling case of collapse than K41. The collapse of the spectrum is robust for the data presented here ($R_\lambda > 50$) in the range $0 < \ln(k\eta)/\ln(R_\lambda) < 0.4$ (loosely covering NDR), but it is also clear that the multifractal description has limited success in the FDR, broadly speaking.

In an attempt to physically understand how the pure exponential of low R_λ assumes a multiexponential form at higher R_λ, we note that the pure exponential simply represents the case when the energy dissipation is proportional to the energy at each of the wave numbers. As the Reynolds number increases, however, there is an intermittent transfer of energy to small scales, potentially from larger scales. This effect becomes increasingly important at increasing wave numbers (though at some truly large wave number, the effects will presumably vanish). This is seen in Fig. 5(a), which shows a time series of the energy spectrum $E(k\eta, t)$, normalized by the median value of the time series $\widetilde{E}(k\eta)$.

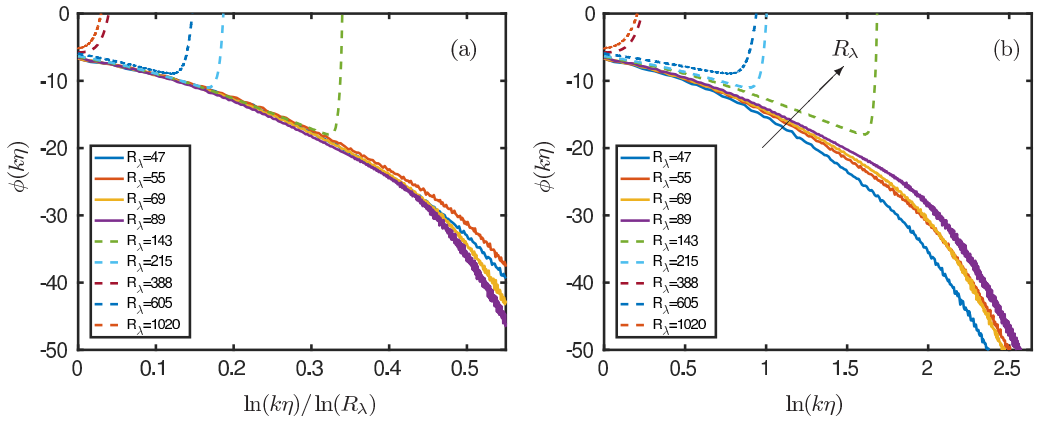

FIG. 4. Log-derivative of the energy spectrum according to the (a) multifractal formalism (see Ref. [18]) and (b) K41 scaling. The range $0 < \ln(k\eta)/\ln(R_\lambda) < 0.4$ corresponds to the so-called intermediate dissipative range [18]. Data for $R_\lambda > 89$ (dashed lines), taken from Ref. [15], correspond to simulations with limited resolution to assess FDR scaling as well-known aliasing errors (seen as a strong uptick in the present normalization) are apparent in the figure.

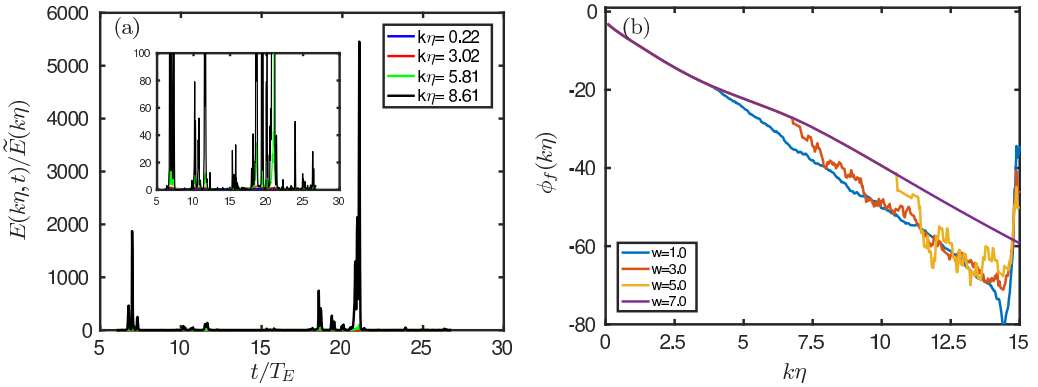

FIG. 5. (a) Time series of energy spectrum $E(k\eta, t)$ normalized by the median value of the time series $\widetilde{E}(k\eta)$ for a subset of wave numbers at $R_\lambda \approx 90$. The inset shows the same data on an expanded scale. (b) Log-derivative of the filtered time average for the energy spectrum, $\phi_f(k\eta)$ for different values of the threshold cutoff w. Data with $w = 7$ were found to correspond to the unfiltered time series.

Large bursts in energy are observed intermittently for high wave numbers. It is thus natural to assess the effect of these intermittent events on the time-averaged energy spectrum. To do so, we remove large bursts by filtering out spectra at time instants where $E(k, t)$ exceeds a chosen threshold; that is, we retain $10^{-w} < E(k, t)/\widetilde{E}(k) < 10^{w}$ in the average for some chosen threshold w. With this so obtained filtered time-averaged spectrum $[E_f(k\eta)]$ one can compute the filtered log-derivative $\phi_f(k\eta)$, shown in Fig. 5(b) for different values of w. The data show that as we remove more of the intermittent events, we essentially recover the low-R_λ exponential, and the difference between NDR and FDR vanishes. This is a clear demonstration that the deviation from the exponential form occurs essentially from bursts of energy transfer. Based on the elementary argument given by Kraichnan [21], it can be argued that extreme fluctuations at high wave numbers are due to large-scale activity. Regardless of their specific origin (a topic by itself warranting further research), extreme energy fluctuations at high wave numbers and high R_λ appear to alter the single exponential representation in the entire dissipative range $k\eta \gtrsim 1$.

In summary, we have used highly resolved DNS data of isotropic turbulence to investigate the dissipative wave-number part of the energy spectrum for a range of R_λ. We have shown that the collapse of the Kolmogorov-scaled spectrum reported in the literature (between $0.13 \lesssim k\eta \lesssim 1$) is an artifact of limited resolution and Reynolds number range. The results presented here (see also Refs. [12,15,22]) demonstrate a systematic R_λ dependence (up to $R_\lambda \sim 2300$ from Ref. [22]) of all resolved scales in the energy spectrum. While we have observed an exponential roll-off for the spectrum of the form Eq. (1) at low R_λ, a systematic analysis of the coefficients involved shows two distinct scaling ranges. A general expression that captures these two regimes can be written as $E(k\eta) \sim e^{\beta_1(k\eta)^{\gamma_1}} + Ae^{\beta_2(k\eta)^{\gamma_2}}$, where $\gamma_2 \sim 1$, $A \ll 1$. This form is not found in traditional formalisms. The second exponential ($\gamma_2 \sim 1$) has been predicted using different approaches but, as we have shown, it is realized at much higher wave numbers than previously considered. The multifractal scaling seems to provide a better representation in the intermediate dissipation range (around NDR), but not at very high wave numbers in the FDR. We have made a connection between the second exponential and intermittent energy transfer. By removing these intense fluctuations (argued to be due to activity in the larger scales by Kraichnan), the spectrum reverts to the single low-R_λ exponential. It is also interesting to note that the two-exponential behavior is observed for $R_\lambda \gtrsim 20$. This Reynolds number is not far from the critical value recently put forth by Yakhot and Donzis [23,24] beyond which moments of velocity gradients and dissipation transition from the Gaussian state to a fully anomalous state characterized by intermittency. A more thorough analysis of this connection is a part of ongoing research.

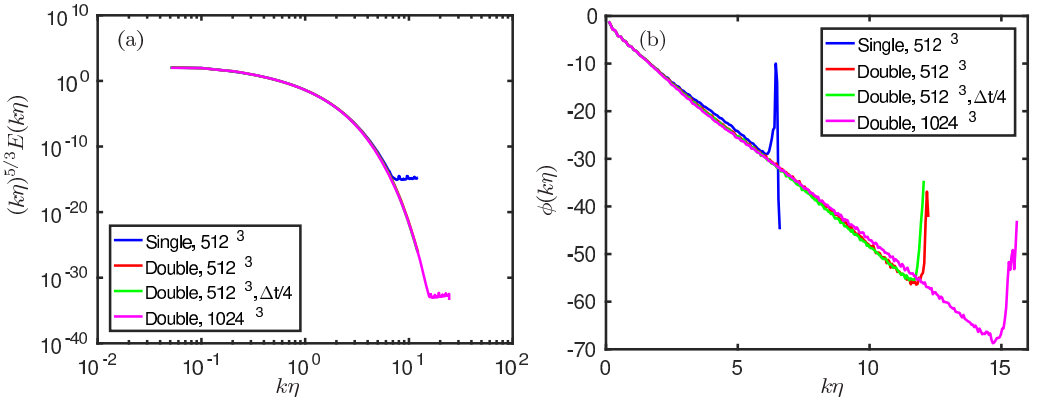

FIG. 6. (a) Energy spectrum and (b) its log-derivative for $R_\lambda \sim 50$.

Finally, this work suggests two more conclusions. First, fitting a single exponential to high-R_λ data may lead to conflicting results as the numerical values of the parameters depend strongly on the range over which the fit is performed as it may cover NDR, FDR, or both. Second, the very large bursts of energy that are observed in FDR present difficulties in time averaging as strong and localized events can be missed or skew the mean. Thus, very long records with a very high time resolution (both perhaps beyond current practices) are needed for converged averages, especially in the FDR.

ACKNOWLEDGMENTS

Support from the Hagler Institute for Advanced studies at Texas A&M University is gratefully acknowledged. This work used supercomputers provided by the Extreme Science and Engineering Discovery Environment (XSEDE) through allocation TG-CTS110029.

APPENDIX

1. Numerical resolution

In order to verify that small scales are not contaminated by numerical artifacts, we have tested for three main sources of errors: small-scale and time resolution, and finite arithmetic precision.

We run a series of simulations at the same conditions but with different resolutions and precision. A typical result is shown in Fig. 6 for which we show both the compensated spectrum and the log-derivative as in Fig. 1. In Fig. 6(a), we see that the three cases overlap with each other up to $k\eta \approx 6$ where the single-precision data (4-byte real) depart with contamination from round-off errors. We have verified this departure to be insensitive to an increase in resolution, as expected if the source is rounded off. The 512^3 case with double precision (8-byte real) extends further without being affected by round-off errors. When the resolution is increased to 1024^3, the spectral content decreases to levels where round-off errors are apparent for this precision at $k\eta \approx 14$. We have also tested time resolution effects. A typical result is shown in the figure as well. We see that reducing the time step for this resolution by a factor of 4 results in no observable changes in the spectrum. Similar conclusions are arrived at from the even more detailed view of these effects in Fig. 6(b).

Thus, we find that doubling the resolution only weakly affects the high-wave-number part of the spectrum, with most of the effects confined around $k \sim O(k_{\max})$, as seen in Fig. 6. This is consistent with the conclusions of Ref. [25], though the authors worked with resolutions $k_{\max}\eta \leqslant 3.8$. In order to observe a FDR, however, one obviously needs a much higher resolution. As an aside, we note that the spectra from Ref. [25] also seem to exhibit a systematic Reynolds number trend for (even marginally) resolved wave numbers in the NDR, consistent with the results presented here. In fact, a

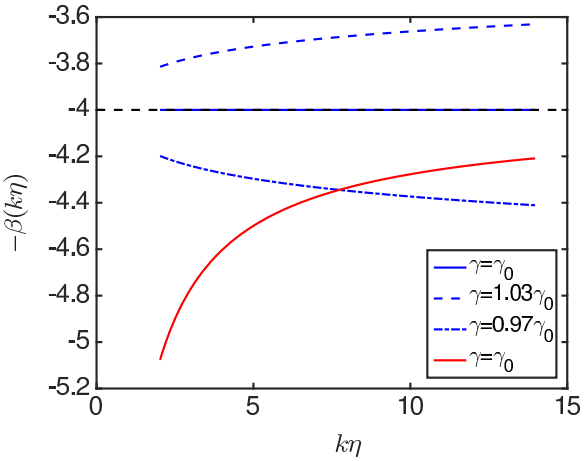

FIG. 7. Compensated curves with over- and underpredicted values for γ. Blue lines are for a pure exponential and the red line is for an exponential prefixed with a power law ($\alpha_0 = -5/3$). Both have $\beta = 4$ (dashed black line) and $\gamma_0 = 0.85$.

careful observation of the spectrum in Refs. [15,16] also shows a slight Reynolds number trend even for $k\eta < 1$. The Reynolds number trend for the FDR reported here can also be seen in Ref. [13].

2. Determination of fitting parameters

Here, we show further tests for the compensation method used to determine the coefficients. As explained in the text, the method is based on obtaining γ as the value that results in the widest plateau for $\phi(x)/(\gamma x^{\gamma})$. To test the accuracy of the method, we use a known function $(k\eta)^{\alpha_0} \exp[\beta_0 (k\eta)^{\gamma_0}]$ with given α_0, β_0, and γ_0 and use our technique based on Eq. (3) to compare the obtained coefficients. In Fig. 7 we show typical results for $(\alpha_0, \beta_0, \gamma_0) = (0, 4, 0.85)$ (blue lines) and $(\alpha_0, \beta_0, \gamma_0) = (-5/3, 4, 0.85)$ (red line). It is clear from Eq. (3) that a wide plateau, with the correct β is, in theory, only observed for the case with no power law ($\alpha_0 = 0$). We look at that case first. In the figure we plot results for γ which is deliberately selected to be 3% below and above the exact value (γ_0). In both cases no plateau is observed and no β could thus be identified. This example shows

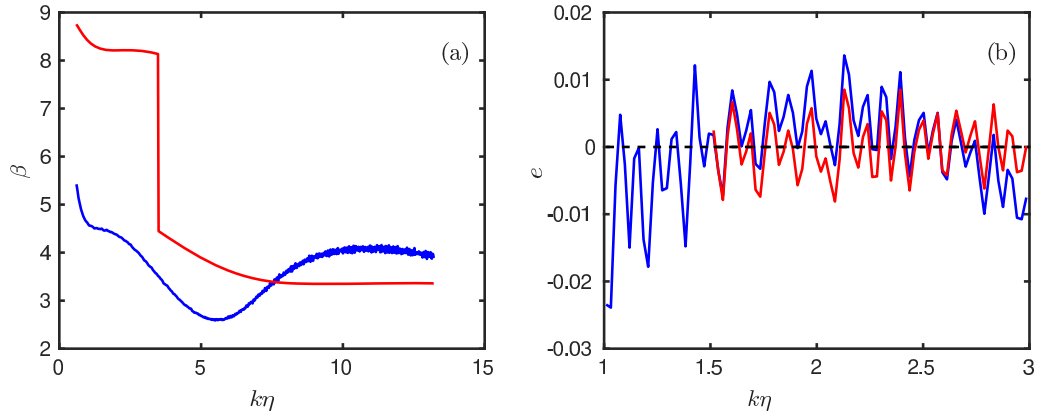

FIG. 8. (a) Value of β when fit locally for $R_\lambda \sim 90$. (b) Relative error between DNS data and Eq. (1) using parameters obtained with the present method (red) and that of Ref. [11] (blue).

how the compensation method is found to be able to visually account for a few percentage points errors in the determination of γ. For the case with a power law ($\alpha_0 \neq 0$), the approach to the right value of β is seen to occur only asymptotically at very large $k\eta$ when the correct γ is used (red line): No plateau is observed in this case. Thus, the plateau observed in DNS data (Fig. 2) is indicative of both an appropriate value of γ and a negligible α, as argued in the text.

We also compare our local fitting procedure with that of Refs. [11,26]. Both studies assumed $\gamma = 1$ and fit locally both α and β. Schumacher *et al.* [26] concluded that no visible asymptotic behavior was observed for his data and that α appears to change sign. Martinez *et al.* [11] used their highest resolved simulation to show that β approaches a constant. However, they could only resolve up to $k\eta \approx 11$. In Fig. 8(a) (blue line) we show a case in our DNS database using their method. What we observe is that β does not approach a constant but instead a local maximum around $k\eta \approx 10$, which may be mistakenly taken as an asymptote if no data at higher wave numbers are available. If instead we use the present method on the same data, we find clear asymptotic behavior in both NDR and FDR (red line). A constant value of β is now observed as the proper value of γ is used and α is not a fitting parameter. We also see that our method results in smoother curves, especially at high $k\eta$. The relative error between DNS and Eq. (1) with parameters obtained by these two methods is shown in Fig. 8(b). An important observation in the figure is that the procedure in Ref. [11] leads to errors with a nonrandom structure: negative error at low and high k and positive error at intermediate k. This is indicative of an inappropriate fitting function, or, in this case, γ values. The method proposed here, instead, leads to a randomly distributed error and with an overall smaller error.

[1] A. N. Kolmogorov, Dissipation of energy in the locally isotropic turbulence, Proc. Math. Phys. Sci. **434**, 15 (1991).

[2] A. S. Monin and A. M. Yaglom, *Statistical Fluid Mechanics* (MIT Press, Cambridge, MA, 1975), Vol. II.

[3] R. H. Kraichnan, The structure of isotropic turbulence at very high Reynolds numbers, J. Fluid Mech. **5**, 497 (1959).

[4] U. Frisch and R. Morf, Intermittency in nonlinear dynamics and singularities at complex times, Phys. Rev. A **23**, 2673 (1981).

[5] K. R. Sreenivasan, On the fine-scale intermittency of turbulence, J. Fluid Mech. **151**, 81 (1985).

[6] C. Foias, O. Manley, and L. Sirovich, Empirical and Stokes eigenfunctions and the far-dissipative turbulent spectrum, Phys. Fluids A **2**, 464 (1990).

[7] O. P. Manley, The dissipation range spectrum, Phys. Fluids A **4**, 1320 (1992).

[8] L. Sirovich, L. Smith, and V. Yakhot, Energy Spectrum of Homogeneous and Isotropic Turbulence in Far Dissipation Range, Phys. Rev. Lett. **72**, 344 (1994).

[9] Z. S. She and E. Jackson, On the universal form of energy spectra in fully developed turbulence, Phys. Fluids A **5**, 1526 (1993).

[10] S. Chen, G. Doolen, J. R. Herring, R. H. Kraichnan, S. A. Orszag, and Z. S. She, Far-Dissipation Range of Turbulence, Phys. Rev. Lett. **70**, 3051 (1993).

[11] D. O. Martinez, S. Chen, G. D. Doolen, R. H. Kraichnan, L. P. Wang, and Y. Zhou, Energy spectrum in the dissipation range of fluid turbulence, J. Plasma Phys. **57**, 195 (1997).

[12] T. Ishihara, Y. Kaneda, M. Yokokawa, K. Itakura, and A. Uno, Energy spectrum in the near dissipation range of high resolution direct numerical simulation of turbulence, J. Phys. Soc. Jpn. **74**, 1464 (2005).

[13] J. Schumacher, Sub-Kolmogorov-scale fluctuations in fluid turbulence, Europhys. Lett. **80**, 54001 (2007).

[14] V. Eswaran and S. B. Pope, An examination of forcing in direct numerical simulations of turbulence, Comput. Fluids **16**, 257 (1988).

[15] D. A. Donzis and K. R. Sreenivasan, The bottleneck effect and the Kolmogorov constant in isotropic turbulence, J. Fluid Mech. **657**, 171 (2010).

[16] T. Ishihara, T. Gotoh, and Y. Kaneda, Study of high-Reynolds number isotropic turbulence by direct numerical simulation K41: Kolmogorov's idea on the universality in the small-scale statistics of turbulence at high Re far away from boundaries, Annu. Rev. Fluid Mech. **41**, 165 (2009).

[17] A. Bershadskii, Distributed chaos in the Hamiltonian dynamical systems and isotropic homogeneous turbulence, arXiv:1803.10139.
[18] U. Frisch, *Turbulence: The Legacy of A. N. Kolmogorov* (Cambridge University Press, Cambridge, UK, 1995).
[19] G. Falkovich, Bottleneck phenomenon in developed turbulence, Phys. Fluids **6**, 1411 (1994).
[20] W. Dobler, N. E. L. Haugen, T. A. Yousef, and A. Brandenburg, Bottleneck effect in three-dimensional turbulence simulations, Phys. Rev. E **68**, 026304 (2003).
[21] R. H. Kraichnan, Intermittency in the very small scales of turbulence, Phys. Fluids **10**, 2080 (1967).
[22] T. Ishihara, K. Morishita, M. Yokokawa, A. Uno, and Y. Kaneda, Energy spectrum in high-resolution direct numerical simulations of turbulence, Phys. Rev. Fluids **1**, 082403(R) (2016).
[23] V. Yakhot and D. Donzis, Emergence of Multiscaling in a Random-Force Stirred Fluid, Phys. Rev. Lett. **119**, 044501 (2017).
[24] V. Yakhot and D. A. Donzis, Anomalous exponents in strong turbulence, Physica D (2018), doi:10.1016/j.physd.2018.07.005.
[25] T. Watanabe and T. Gotoh, Inertial-range intermittency and accuracy of direct numerical simulation for turbulence and passive scalar turbulence, J. Fluid Mech. **590**, 117 (2007).
[26] J. Schumacher, K. R. Sreenivasan, and V. Yakhot, Asymptotic exponents from low-Reynolds-number flows, New J. Phys. **9**, 89 (2007).